scientific reports

OPEN

Mathematical model of oxygen minimum zones in the vertical distribution of oxygen in the ocean

Yazeed Alhassan[1]✉, Ivo Siekmann[2] & Sergei Petrovskii[3,4]✉

Processes determining the amount and spatial distribution of dissolved oxygen in the ocean have been a focus of intense research over the last two decades. Anomalies known as Oxygen Minimum Zones (OMZs) have been attracting growing attention, in particular because their growth is believed to be a result of the global environmental change. Comprehensive understanding of factors contributing to and/or controlling the emergence and evolution of OMZs is still lacking though. OMZs are usually thought to result from an interplay between the oxygen transport through the water column from the ocean surface and variable oxygen solubility at different water temperature. In this paper, we suggest a different, novel mechanism of the OMZ formation relating it to the oxygen production in phytoplankton photosynthesis in a stratified ocean. We consider a simple, conceptual model of the coupled phytoplankton-oxygen dynamics and show that the model predictions are in qualitative agreement with some relevant field observations.

**Keywords** OMZ, Phytoplankton, Photosynthesis, Turbidity

Dissolved oxygen is one of the most important factors that determines the health of marine environment. Concentration of dissolved oxygen to a large extent controls the well-being, distribution and spatiotemporal dynamics of essentially all aquatic organisms[1–6]. A decrease in the oxygen level below a certain threshold can lead to a mass mortality of marine fauna with catastrophic consequences for the corresponding marine ecosystem[7].

Spatial distribution of the dissolved oxygen is often distinctly heterogeneous both in horizontal and vertical directions[8–11]. Whilst at some locations the water can be well oxygenated, at another location nearby the oxygen level may be close to or even below the hypoxic threshold ($\leqslant 2$ mg l^{-1}). A typical example is shown in Fig. 1. One readily observes that, both in the subsurface level or at any given depth, the oxygen concentration varies considerably along the horizontal transect. Even greater heterogeneity is observed in the vertical distribution where the variations in oxygen level can reach 200–300%, with well oxygenated water near the ocean surface and at large depths but falling into hypoxic or anoxic conditions at intermediate depths between 500 and 1000 m.

Analysis of this and many other similar cases, e.g. see[12,13], reveals that the oxygen vertical distribution often exhibits a clearly defined structure. Namely, water column can be divided into four parts or layers[14], as is conceptualised in Fig. 2. They are (i) the well-oxygenated layer near the ocean surface, (ii) a relatively thin layer further down where oxygen concentration sharply declines ('oxycline'), (iii) a core layer where oxygen levels are at their minimum concentration, and finally (iv) the well oxygenated waters at large depth. Correspondingly, the core layer where the oxygen level exhibits its minimum (often resulting in anoxic or hypoxic conditions) is called the Oxygen Minimum Zone (OMZ).

The existence of OMZ has a profound effect on the marine species abundance and the aquatic trophic web as a whole, and that becomes an urgent priority for research[15]. The significant drop in the dissolved oxygen level eventually results in the formation of a dead zone, so that the majority of marine life either dies or leaves the area[2,16,17]. Moreover, there is growing evidence that OMZs are expanding in response to the climate change[2,7,13,16,18]. For these reasons, OMZs in different parts of the world ocean have been a focus of attention and intense empirical and theoretical/modelling research over the last two decades[18–26]. However, while considerable emprirical work has been done and large amount of data have been collected, a good understanding of the mechanisms resulting in the formation of OMZ and/or controlling their size and location is still lacking.

[1]Mathematics Department, College of Science, Jouf University, P.O. Box 2014, Sakaka, Saudi Arabia. [2]School of Computer Science and Applied Mathematics, Liverpool John Moore University, Liverpool, UK. [3]School of Computing and Mathematical Sciences, University of Leicester, Leicester LE1 7RH, UK. [4]Peoples Friendship University of Russia (RUDN University), 6 Miklukho-Maklaya St., Moscow 117198, Russian Federation. ✉email: yazeed1921@hotmail.com; sp237@le.ac.uk
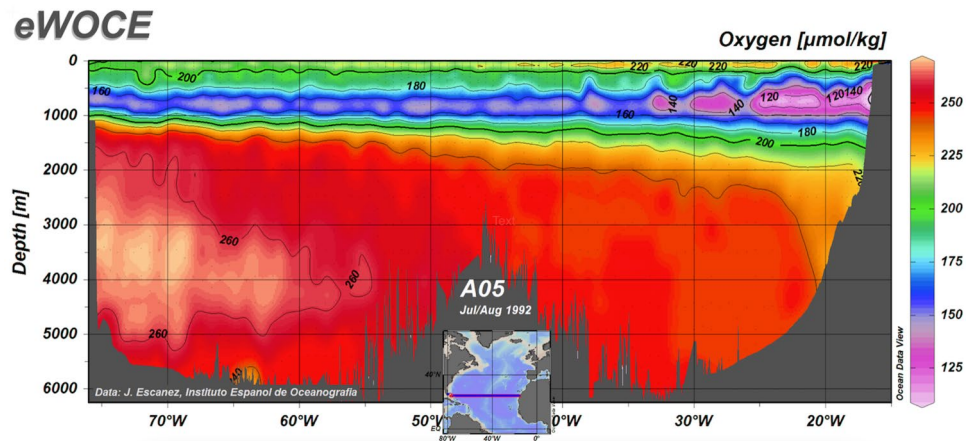
Fig. 1. Dissolved oxygen profile from a transect across the Atlantic Ocean from Florida to the coast of Africa (as in the inset). The oxygen minimum layer is visible between 500–1000 m. Adapted from[6].
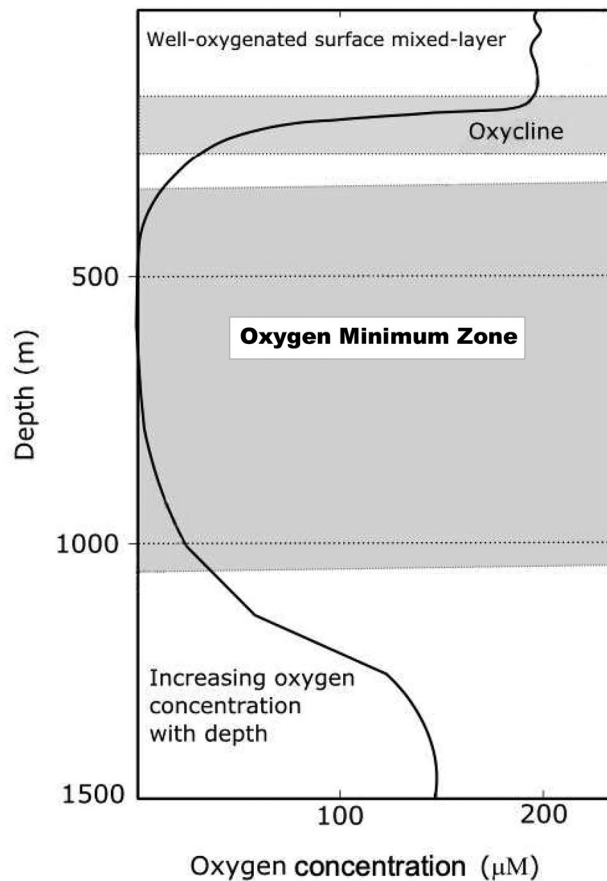
Fig. 2. Typical structure of the oxygen vertical distribution in case of OMZ. Black curve shows the concentration of dissolved oxygen. Adapted from[14].

Dissolved oxygen contained by the ocean waters mainly originates from two sources. Firstly, it can come from the atmosphere through the ocean-air interface. This is commonly considered as the main factor controlling the levels of dissolved oxygen, as the well oxygenated water from under the ocean surface is eventually transported both horizontally and vertically through the water column with eddies and by turbulent mixing[9,21,27,28].

Correspondingly, the formation of OMZ has often been attributed to the effect of hydrological and hydro-physical factors, in particular to the interplay between the specifics of vertical mixing, stratification, and oxygen solubility, i.e. the fact that the maximum oxygen concentration that water can contain (i.e., at saturation)

decreases with an increase in the water temperature. Together with other effects of ocean warming (in particular, an increased stratification of the upper ocean[29,30]), the latter may lead to hypoxia[7], which in turn often leads to an elevated mortality of marina fauna and considerable biodiversity loss[31–34].

Secondly, dissolved oxygen is produced in the photosynthetic activity of aquatic plants, in particular phytoplankton. Dependence of the dissolved oxygen on the photosynthesis rate is well know and well studied e.g. see[31]. There is a vast literature on various aspects of the dependency of dissolved oxygen on the spatial distribution of phytoplankton[35–38]. A decrease in the rate of oxygen production by phytoplankton may have catastrophic results. Moreover, on the global scale photosynthesis is ultimately responsible for the total Earth's O_2 budget. It is estimated that phytoplankton has produced about two-thirds of the present stock of atmospheric oxygen[39].

We mention here that, as long as photosynthesis is concerned, availability of sunlight is the main resource for the oxygen production. Sunlight is absorbed by water, so that its intensity decays approximately exponentially with the depth[40]. The euphotic zone in the oceans is usually up to 200 m deep, although the depth varies[41]. Also, the amount of solids (e.g. micro-plastic) and other light-scattering elements in water determines how deep the euphotic zone actually is. Correspondingly, turbidity is a primary controlling factor[42].

Surprisingly, the apparent link between oxygen concentration and photosynthesis (and hence phytoplankton density and the conditions facilitating photosynthesis such as availability of sunlight) remains under-investigated as a factor potentially responsible for the formation of OMZs. Even that some modelling studies had included photosynthesis as a part of their biochemical box[20,22,26], the formation and dynamics (e.g. seasonal and inter-annual variations) of OMZ are always attributed to the effect of ocean transport processes, mainly due to mesoscale eddies. In particular, possible effect of water turbidity on the position and extent of OMZ has been largely overlooked. A recent study by Bettencourt et al.[25] had a clearer focus on the effect of photosynthesis in the oxygen distribution over the water column; however, their simulation results only predicted a monotone decrease in the oxygen concentration, hence not describing an OMZ where the decrease in the dissolved oxygen at intermediate depth is followed by its increase at a larger depth (see Fig. 2). A question therefore arises as to what can be a 'minimal system' allowing for formation of OMZ, in particular whether the transport with mesoscale eddies is really an essential part of it.

This paper aims at bridging this gap, at least partially. Namely, we develop a conceptual mathematical model that shows that the OMZ is, to some extent, an intrinsic property of photosynthetic oxygen production in a stratified water column. Our results are in a good qualitative agreement with some observations.

Mathematical model

In order to describe oxygen production and distributions in the ocean, we consider a conceptual, compartment-type model of coupled phytoplankton-oxygen dynamics consisting of two components ('compartments'), i.e. dissolved oxygen and phytoplankton; see Fig. 3. Let u be the phytoplankton density and c be the concentration of dissolved oxygen. Oxygen is produced by phytoplankton with rate $P(u, c)$ during the day time when there is sunlight. Oxygen is consumed, as required for phytoplankton 'breathing' (i.e. metabolism), with rate $Q(u, c)$ during the night when there is no light; thus, the rate of the net oxygen production is $(P - Q)$. Phytoplankton grows with rate $G(c, u)$ and dies with a certain mortality rate $M(u)$. A fraction of oxygen is 'wasted' with rate $W(c)$, i.e. consumed in the processes not included into the model explicitly, e.g. used for breathing by marine fauna, used in biochemical reactions, etc.

This conceptual system can be expressed mathematically as follows:

$$\frac{dc}{dt} = P(u, c) - Q(u, c) - W(c), \tag{2.1}$$

$$\frac{du}{dt} = G(u, c) - M(u), \tag{2.2}$$

where all the terms in the right-hand side are explained above.
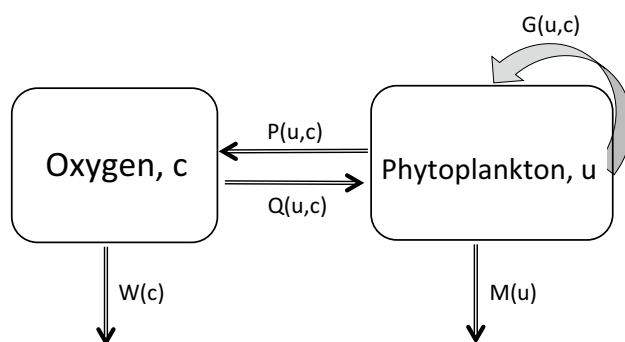
Fig. 3. Flow chart representation of the conceptual phytoplankton-oxygen model. Arrows show mass flows in the system; see details in the text.

Based on some available data as well as general understanding of the processes involved, the functions in system (2.1-2.2) can be parameterized, so that Eqs. (2.3-2.4) take the following more specific form[43]:

$$\frac{\partial c(z,t)}{\partial t} - D\frac{\partial^2 c}{\partial z^2} = \frac{Au}{c+1} - \frac{\delta uc}{c+c_2} - c, \tag{2.3}$$

$$\frac{\partial u(z,t)}{\partial t} - D\frac{\partial^2 u}{\partial z^2} = \left(\frac{Bc}{c+c_1} - u\right)u - \sigma u, \tag{2.4}$$

(in dimensionless units) where we have also included explicit spatial dependence. Here $c = c(z,t)$ and $u = u(z,t)$ are, respectively, the concentration of oxygen and the density of phytoplankton at time t and depth z. The diffusion terms account for vertical mixing, D being the coefficient of turbulent diffusion[44]; in dimensionless units $D = 1$, see Supplementary Information for details. The first term in the right-hand side of Eq. (2.3) describes the oxygen production (for details, please see[43]), parameter A being the average oxygen production rate per cell. The second term describes oxygen consumption by phytoplankton required for its own metabolism; parameter δ quantifies the rate of oxygen consumption and c_2 is the half-saturation constant. The last term in Eq. (2.3) accounts for the 'waste' of oxygen because of its use in other processes not included explicitly into the model (e.g decay of the organic matter). In the right-hand side of Eq. (2.4), the first term describes the phytoplankton growth, which is assumed to be logistic type, where the square term accounts for intraspecific competition. Parameter B is the linear growth rate in the large-oxygen limit (i.e. under well oxygenated conditions) and parameter c_1 quantifies the oxygen threshold density when oxygen becomes a factor limiting the phytoplankton growth. The last term describes the phytoplankton natural mortality. All variables and parameters in Eqs. (2.3-2.4) are dimensionless (see Supplementary Information); for details of the derivation of Eqs. (2.3-2.4), see[43].

Note that, in the model (2.3-2.4), the oxygen production rate A is regarded as a parameter. However, the oxygen production rate depends on a number of environmental factors, in particular on the availability of sunlight. In turn, the intensity of sunlight (say I), as was discussed in the introduction, depends on the depth in the water column, decaying approximately exponentially, i.e. $I(z) = I_0 \exp(-\gamma z)$ where I_0 is the maximum light intensity reached at the ocean surface (at $z = 0$) and coefficient γ quantifies the decay rate. Exact relation between the sunlight intensity and the rate of photosynthesis is unknown but, since sunlight is the main limiting factor, A is a monotonously increasing function of I. Assuming that A is proportionate to I, we obtain that the rate of oxygen production is also an exponential function of the depth:

$$A(z) = ae^{-\gamma z}, \tag{2.5}$$

where a is the maximum oxygen production rate reached in the ocean layer immediately below the surface.

To further extend the baseline model, we recall that, in the context of plant physiology (including phytoplankton), the main purpose of photosynthesis is to produce sugars, oxygen being produced merely as a by-product. It means that a certain minimum amount of sunlight is necessary for the plant survival. Since the intensity of sunlight decays with water depth, it means that there must exist a certain critical depth, say L_*, below which phytoplankton cannot survive. It does not of course mean that water at the depths $z > L_*$ are lacking any life, as there are a number of species that use chemosynthesis instead of photosynthesis. Importantly, however, chemosynthesis does not produce oxygen. Altogether, it means that the model (2.3-2.4) as such is only valid for $z < L_*$ while for depths $z > L_*$ it reduces to merely transport equations accounting for the effect of vertical mixing:

$$\frac{\partial c(z,t)}{\partial t} = D\frac{\partial^2 c}{\partial z^2} - \epsilon c, \quad z > L_* \tag{2.6}$$

$$\frac{\partial u(z,t)}{\partial t} = D\frac{\partial^2 u}{\partial z^2} - \sigma u, \quad z > L_*. \tag{2.7}$$

Note that the above system formally still contains the equation for phytoplankton. Indeed, although phytoplankton is unable to reproduce and survive at $z > L_*$, it can be brought there by vertical mixing. Whenever this happen, it will eventually die at a rate σ. The last term in Eq. (2.6) has the same meaning as in Eq. (2.3), assuming additionally that $\epsilon \ll 1$.

Thus, our mathematical model of the phytoplankton-oxygen dynamics in a deep water column consists of Eqs. (2.3-2.4) (with $A(z)$ given by (2.5)) for the upper part of the column, $0 < z < L_*$, and Eqs. (2.6-2.7) for the lower part of the column, $z > L_*$.

We mention here that, strictly speaking, parameters L_* and γ are not entirely independent, as both of them refer to the same phytoplankton ability to perform photosynthesis. However, any relation between them is by no means straightforward. Indeed, it is well known that the rate of photosynthesis depends not only on the availability of light but also on a number of other environmental factors such as temperature, availability of CO_2, availability of nitrogen, etc.[45]. In a multi-species phytoplankton community, it can also depend on the taxonomic composition and physiological state of populations[46]. It means that, in a real-world plankton-oxygen system, for the same value of γ, the water depth where the photosynthesis actually stops can differ significantly. Since our "minimal model" does not explicitly account for any of the above factors except for sunlight, it seems reasonable to assume that L^* and γ are independent.

Simulation results

System (2.3)-(2.7) is solved numerically in the spatial domain $[0, L_{max}]$, i.e. in a water column that extends from the surface (at $z = 0$) to the seabed (at depth L_{max}). At the domain boundaries, we use the 'no-flux' Neumann boundary conditions, that is

$$\text{(a)} \quad \frac{\partial c(t, z = 0)}{\partial z} = 0, \qquad \text{(b)} \quad \frac{\partial c(t, z = L_{max})}{\partial z} = 0, \tag{3.1}$$

and

$$\text{(a)} \quad \frac{\partial u(t, z = 0)}{\partial z} = 0, \qquad \text{(b)} \quad \frac{\partial u(t, z = L_{max})}{\partial z} = 0. \tag{3.2}$$

The meaning of the boundary conditions (3.2) is obvious: phytoplankton cannot penetrate through the ocean bed and cannot leave the water through the ocean-air interface; hence, there is no flux. For oxygen, however, it is less straighfoward. Dissolved oxygen can, in principle, diffuse through the ocean bed but the corresponding flux is likely to be very small. We consider it zero, which leads to Eq. (3.1b). At the other end ($z = 0$), oxygen definitely can diffuse through the ocean surface; this is an essential component of the ocean-atmosphere exchange[47–49]. The corresponding oxygen flux exhibits considerable variability both in time (on multiple timescales, in particular, seasonal and multi-annual[47,49]) and in space[48], showing a different magnitude and a different sign (i.e. with the predominant direction in or out of the ocean). However, the total flux (i.e. integrated over the total surface of the world ocean) was shown to be not significantly different from zero[48]. The interannual variability of the total flux can be affected by global climate trends. Correspondingly, on a shorter timescale, e.g. before the global climate change brings any significant changes to the average Earth surface temperature, the mean value of the oxygen flux is likely to be very small. For the sake of simplicity we assume it to be zero, thus arriving at the boundary condition (3.1a).

In order to perform numerical simulations, we have to assume certain numerical values for the model parameters; see Table 1. We mention here that, since our model is conceptual, i.e. it is designed to explain tendencies in the dissolved oxygen distribution but not necessarily specific values of the oxygen concentration at specific depths, we are not attempting to use 'realistic' parameter values corresponding to any specific marine ecosystem or any particular ocean conditions. The parameter values that we used in simulations are therefore hypothetical.

Before we proceed to presenting our simulation results, it is worth having a brief look at the properties of the corresponding nonspatial system (i.e. Eqs. (2.3-2.4) without diffusion terms, with c and u depending only of time), as it provides a useful framework for understanding the spatially explicit system. As shown in[43], the nonspatial system always possesses the trivial "extinction" state $(0, 0)$, which is always stable. The oxygen production rate appears to be a bifurcation parameter, so that, for $A > A_{min}$, where A_{min} is a certain threshold value, there also exists a stable positive equilibrium $(\hat{c}, \hat{u})$. These properties are summarised in Fig. 4. Thus, in order to ensure that phytoplankton and oxygen can persist, we need to parametrise $A(z)$ (see (2.5)) in such a way so that $A(z) > A_{min}$ at least in some part of the spatial domain. For the parameter set used in simulations (see Table 1), $A_{min} \approx 0.937$. Correspondingly, we choose $a = 2$, which implies that at the surface $A(0) = 2 > A_{min}$.

Emergence of persistent OMZ

Equations (2.3)-(2.4) and (2.6)-(2.7) must be complemented with initial conditions, i.e. $c(z, 0)$ and $u(z, 0)$. The choice of initial conditions is a subtle issue, as different initial conditions may correspond to a different research question and/or to different ecological situations. Our first and main research question in this paper is whether the formation of OMZ can be a property of the photosynthetic oxygen production in the heterogeneous (stratified) ocean. In mathematical terms, it means whether it is an intrinsic property of the model (2.3)-(2.7), where "intrinsic property" means that the model solution with relevant properties (i.e. showing a gap in the oxygen

Parameter	Meaning	Numerical value
a	Maximum oxygen production rate	2.0
γ	Decay rate of light	$9 \cdot 10^{-4}$
L_*	Threshold depth of light availability	10^3
B	Plankton maximum linear growth rate	1.8
c_1	Half-saturation constant of oxygen consumption	0.7
σ	Phytoplankton natural mortality rate	0.1
δ	Maximum respiration rate	1.0
c_2	Half-saturation constant of phytoplankton growth	1.0
ϵ	Oxygen decay rate in deep ocean	0
D	Coefficient of vertical diffusivity	1

Table 1. Dimensionless parameters of the model (2.3)-(2.7). See Supplementary Information for details of adimensionalisation procedure.
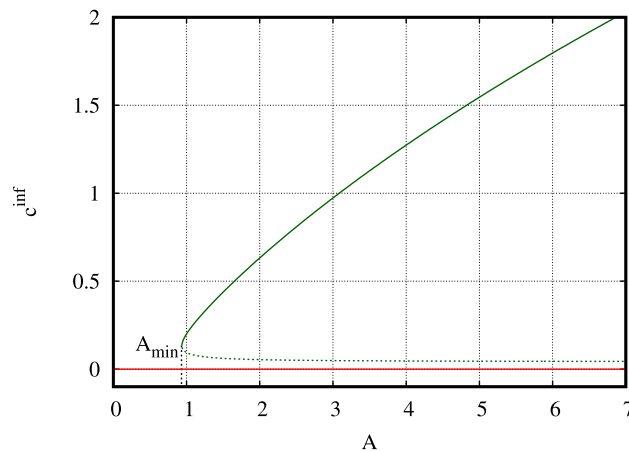
Fig. 4. Bifurcation diagram for the non-spatial version of model (2.3)-(2.4) showing the steady state values of oxygen concentration $\hat{c}$ as a function of the oxygen production rate. Other parameters are given in Table 1. For $A < A_{min} \approx 0.937$, there exists only the trivial 'extinction' solution, $(\hat{c}, \hat{u}) = (0, 0)$ (red line), which is always stable. For $A > A_{min}$, there are also two positive steady states, one of the stable (solid green curve), the other unstable (dotted black curve).

distribution at some intermediate depths) must not be too sensitive to the choice of the initial conditions. Correspondingly, to answer our first research question, we consider the initial condition in the following form:

$$c(z, 0) = c_0, \tag{3.3}$$

$$u(z, 0) = \begin{cases} u_0, & \text{if } z < L_*, \\ 0, & \text{if } z > L_*, \end{cases} \tag{3.4}$$

where c_0 and u_0 are certain constants. Note that, since waters in the deep ocean are known to be well oxygenated[6,50,51], the oxygen concentration for $z > L_*$ is taken to be positive ($c_0 > 0$). However, the phytoplankton density at sufficiently large depth ($z > L_*$) is assumed to be zero, as there is not enough light there to support its metabolic processes.

The complete mathematical model (2.3)-(2.7) with (3.1)-(3.4) was solved numerically. We obtained that the transient solution ($c(z, t)$, $u(z, t)$) of the system, converge, in the large-time limit, to a stable stationary solution ($\hat{c}(z), \hat{u}(z)$). Typical spatial profiles of the oxygen concentration and the phytoplankton density emerging in the course of time are shown in Fig. 5. One readily observes apparent resemblance between the shape of the simulated oxygen profile (blue curve in Fig. 5) and that seen in real ocean (cf. Figs. 1 and 2), namely, the gap in the oxygen concentration at some intermediate depth. We mention here that the shape of the profile does not depend on the choice of the initial distribution parameters c_0 and u_0. Moreover, it is also rather robust to variations of other model parameters (as in Table 1).
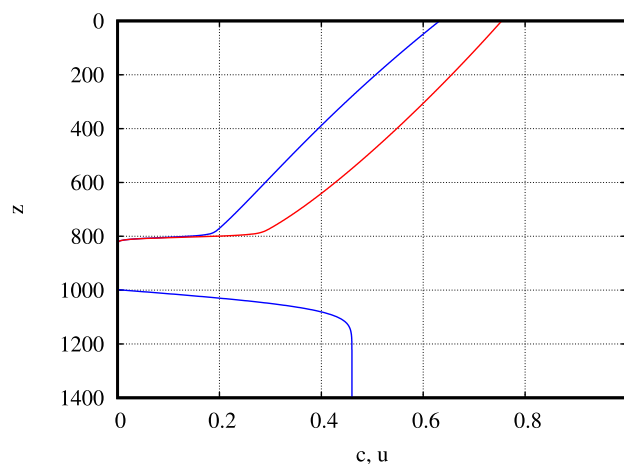
Fig. 5. Steady state profiles of the oxygen concentration (blue line) and the phytoplankton density (red line) vs water depth (in dimensionless units) obtained in the model (2.3)-(2.7). Parameters are given in Table 1.

From a mathematical point of view, the OMZ emerging in our model (2.3)-(2.7) is an interval where the oxygen concentration falls below a certain small value, say c_{min}, that is

$$\mathcal{D} = (z^{\mathrm{T}}, z^{\mathrm{B}}), \text{ such that, for } z^{\mathrm{T}} < z < z^{\mathrm{B}}, \text{ we have } \hat{c}(z) < c_{min}. \tag{3.5}$$

Correspondingly, the size (vertical extent) of OMZ can be defined as the length of the interval, i.e.

$$s(\mathcal{D}) = z^{\mathrm{B}} - z^{\mathrm{T}}. \tag{3.6}$$

An interesting question is how the size of OMZ may depend on environmental parameters. Since in our model the only source for the dissolved oxygen is phytoplankton photosynthesis, availability of light at different depths, quantified by the rate γ of the sunlight decay, is arguably the most relevant factor. In turn, the rate of decay can be regarded as a proxi for water turbidity. Interestingly, a possibility of relation between turbidity and the size and/or location of OMZ was mentioned in the literature[52–54] but no specific dependence was suggested.

In order to make an insight into the above issue, we performed numerical simulations for different values of γ. Results are shown in Fig. 6. It is readily seen that, while the lower bound (z^{B}) of OMZ practically does not change with γ (its value always being close to L_*), the position of upper bound shifts upwards significantly along with an increase in γ. Thus, our model predicts that the size of OMZ increases with an increase in water turbidity, especially in the upper (euphotic) layer.

In conclusion to this section, we mention that the position of the upper bound of OMZ can be estimated analytically. Indeed, by taking into account that the positive stationary solution $(\hat{c}(z), \hat{u}(z))$ loses stability for $A(z) < A_{min}$, we conjecture that the upper bound z^{T} of OMZ is determined by the solution of the equation $A(z^{\mathrm{T}}) = A_{\min}$. Solving it for z^{T}, we readily obtain:

$$z^{\mathrm{T}}(\gamma) = \log(a/A_{\min})/\gamma. \tag{3.7}$$

Correspondingly, we arrive at the following simple estimate for the size of OMZ:

$$s(\mathcal{D})(\gamma) = L_* - \log(a/A_{\min})/\gamma. \tag{3.8}$$

Function $z^{\mathrm{T}}(\gamma)$ appears to be in good agreement with numerical results (see Fig. 6).

Transient OMZ at variable depths

In this section, we are going to explore a different possible scenario for the OMZ formation. It is widely accepted that the dynamics of marine systems is to a large extent driven by random or stochastic factors[55–57]. Obvious examples of the processes that can be regarded as random are given by marine turbulence and the weather fluctuations, but there are many more. Thus, one may ask a question as to whether OMZ can be affected by or resulting from random processes in the ocean dynamics.

Correspondingly, here we consider a hypothetical scenario where, at a certain moment of time, the OMZ emerges as a result of a large fluctuation in the oxygen distribution. The questions then arise as to (i) whether such 'random' OMZ is going to be persistent or transient and (ii) in case of the latter, for how long the OMZ is going to exist and what factors affect the duration of its existence.
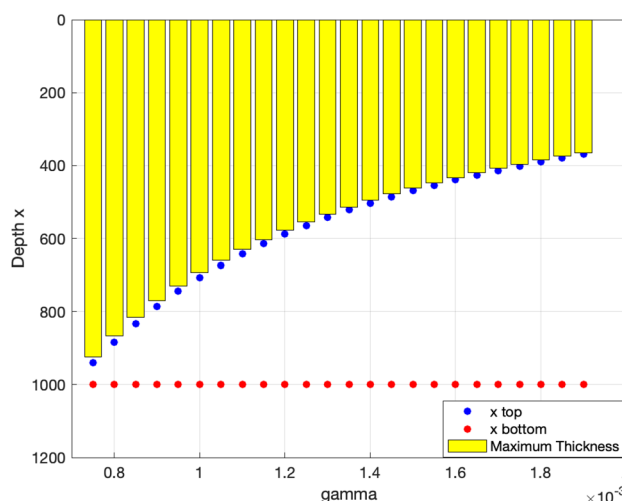
Fig. 6. The structure of the water column (in dimensionless units) obtained for different values of the oxygen decay rate γ, which is a proxi for water turbidity. The yellow bars show well oxygenated water at the top part of the column (where the position of the lower end of the bars is obtained analytically from Eq. (3.7)). Blue and red dots (obtained numerically for $c_{min} = 0.01$, see (3.5)) show, respectively, the top (z^T) and bottom (z^B) boundaries of the OMZ. Apparently, the size of the OMZ grows with water turbidity.

In order to make an insight into the above questions, we perform numerical simulations in the model (2.3-3.2) using the initial conditions of a different type, namely:

$$c(z, 0) = \begin{cases} c_0, & \text{for } 0 \leq z \leq L^{\mathrm{T}} \text{ and } z \geq L^{\mathrm{B}}, \\ 0, & \text{for } L^{\mathrm{T}} < z < L^{\mathrm{B}}, \end{cases} \tag{3.9}$$

and

$$u(z, 0) = \begin{cases} u_0, & \text{for } 0 \leq z \leq L^{\mathrm{T}} \text{ and } L^{\mathrm{B}} \leq z \leq L_*, \\ 0, & \text{if } L^{\mathrm{T}} < z < L^{\mathrm{B}} \text{ and } z > L_*. \end{cases} \tag{3.10}$$

Thus, the initial conditions (3.9)-(3.10) describe an OMZ that exists at $t = 0$. The OMZ position is described by its upper and lower boundaries, i.e. L^{T} and L^{B}, respectively. Note that, contrary to the previous section where the OMZ upper and lower bounds emerged in the course of the evolution of the initial conditions (3.3-3.4), hence being intrinsic properties of system's self-organised dynamics, now L^{T} and L^{B} are parameters. Since availability of light decreases with the depth, one can expect that the evolution of the initial OMZ can be somehow different depending on its position in the water column. Correspondingly, we performed simulations for three different cases: (i) a shallow OMZ with $L^{\mathrm{T}} = 200$ and $L^{\mathrm{B}} = 400$, (ii) an intermediate OMZ with $L^{\mathrm{T}} = 400$ and $L^{\mathrm{B}} = 600$ and (iii) a deep OMZ with $L^{\mathrm{T}} = 600$ and $L^{\mathrm{B}} = 800$.

Our numerical results reveal that, in the large-time limit, the spatial distributions of oxygen and phytoplankton always converge to the stationary profile shown in Fig. 5. However, the transient stage can be rather different, in particular the duration of the existence of the initial OMZ can differ significantly.

Figure 7 shows the distribution of oxygen and phytoplankton in the water column obtained at different time for the cases of shallow, intermediate and deep initial OMZ (left, middle and right columns in Fig. 7, respectively); other parameters are given in Table 1. We readily observe that the 'final', persistent OMZ (which is a part of the stationary solution arising in the large-time limit, cf. Fig. 6) is formed at the location $800 < z < 1000$ at a relatively short time. In all three cases, it is clearly seen already at $t = 150$ (the upper row in Fig. 7). Thus, at this moment, the structure of the water column contains two different OMZs: the lower one (emerged in the course of system's dynamics) and the upper one (prescribed by the initial conditions). The lower one is persistent but the upper one eventually shrinks and disappears, albeit at different time: in the shallow case, it is entirely gone already by $t = 250$ but in the deep case it is still seen at $t = 450$.
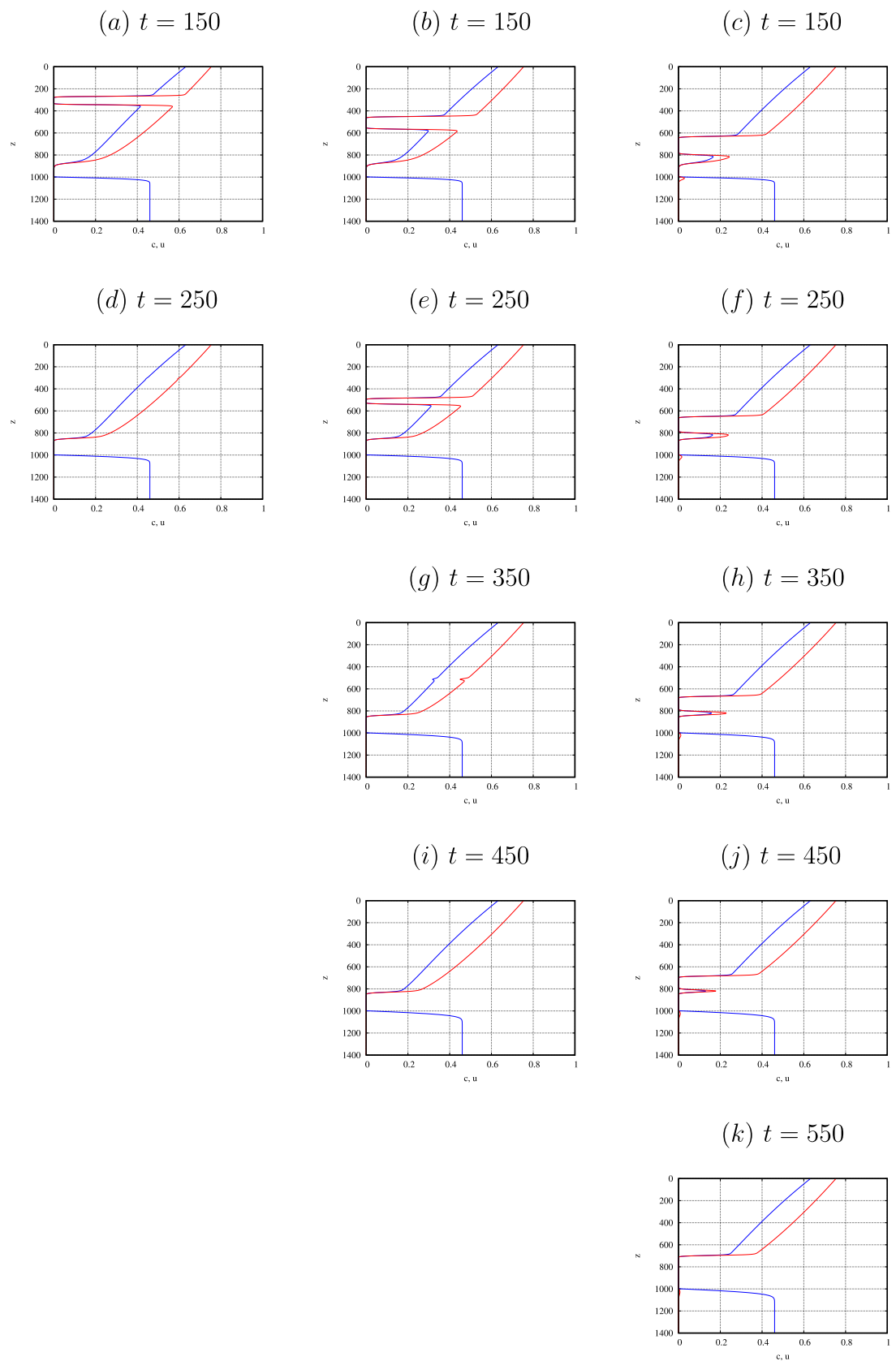
Discussion and conclusion

Dissolved oxygen is a factor that to a large extent determines the health of marine ecosystems, as its depletion may have a detrimental effect on marine fauna leading to mass mortality of animal species[7,15,16]. Understanding factors that can affect the oxygen level and its distribution in the ocean is therefore very important[4,11]. Over the last few decades, considerable attention was attracted by the phenomenon called Oxygen Minimum Zone[1,8,12,13]: the formation in some parts of the world ocean a specific structure of the water column where the concentration of dissolved oxygen falls, at a certain intermediate depth, to a small value creating hypoxic or anoxic conditions (cf. Figs. 1 and 2). The phenomenon was investigated in many empirical and modelling studies; however, a good understanding of the processes responsible for the OMZ formation is still lacking. OMZs are usually attributed to specifics of ocean mixing, in particular to the effect of mesoscale eddies on ventilation, that shapes the oxygen transport both vertically (e.g. from the ocean surface down through the water column) and laterally, connecting waters that are rich and poor with dissolved oxygen level[9,21,22,24,27]. However, although mixing is undoubtfully important, here we argue that there can be other mechanisms. Oxygen is not only transported through the water column, it is also produced by phytoplankton. Although oxygen production in photosynthesis has indeed been accounted for in some modelling studies[20,22,24,26,27], its effect on the OMZ properties has never been distinguished from that of ocean transport. Correspondingly, as photosynthesis is controlled by the availability of sunlight, the potentially important effect of water turbidity on the OMZ position and/or extent has been largely overlooked.

In this paper, our goal was to distinguish the effect of photosynthesis from that of ocean transport with mesoscale structures (e.g. eddies). We therefore have built a kind of 'minimal model' of oxygen-plankton dynamics (see "Mathematical model" section) where the transport is described very schematically, essentially reducing it to the turbulent mixing. Oxygen production, on the contrary, is described in a slightly more realistic way by including the exponential decay of the light intensity with the depth. That results in ocean stratification separating the upper euphotic layer from the 'dark' water below. The rate of light decay (and hence the thickness of the euphotic layer) is known to depend on concentration of micro-particles and thus on water turbidity. We have further hypothesized that, at least in some cases, an OMZ can emerge just as an intrinsic property of the coupled phytoplankton-oxygen dynamics in the ocean stratified according to the light availability.

Having analysed the properties of the model and by performing extensive numerical simulations, we obtained the following main results:

1. In certain situations (in particular, if water turbidity is not too low), an OMZ emerges in the course of system's dynamics regardless of the initial conditions. Such OMZ is persistent: once it has emerged, it will exist for an indefinitely long time. The size of OMZ and the position of its upper bound are estimated analytically (cf. Eq. 3.8) to reveal the effect of turbidity (see Fig. 6);

2. In case the OMZ is regarded as a perturbation of the initial vertical oxygen distribution (e.g. as a large fluctuation resulting from the effect of stochastic factors), it appears to be transient and eventually disappears in the course of time. However, the time of its existence can be long depending on the depth where it is originally

(a) $t = 150$

(b) $t = 150$

(c) $t = 150$

(d) $t = 250$

(e) $t = 250$

(f) $t = 250$

(g) $t = 350$

(h) $t = 350$

(i) $t = 450$

(j) $t = 450$

(k) $t = 550$

Fig. 7. Evolution of a transient OMZ simulated for three different initial depths (in dimensionless units): left, middle and right columns for shallow, intermediate and deep, respectively.

located. In this case, the water column can show, over a certain period of time, a more complicated structure consisting of two OMZs, one stationary and the other transient.

With regard to the first point, several papers mentioned turbidity as a factor relevant to the OMZ formation and evolution[52–54] but no specific relation between turbidity and the OMZ size and position in the water column was suggested. Thus, to the best of our knowledge, our study is the first of its kind to provide a theoretical insight into this issue. Moreover, our theoretical finding that the OMZ size should be an increasing function of the sunlight decay rate (cf. Fig. 6) makes a ground for understanding the effects of other environmental factors and further predictions. For instance, turbidity is known to increase in the presence of micro-particles in the water. In the case where such micro-particles appear as result of some specific forms of pollution (e.g. pollution with micro-plastic[58,59]), an increase in turbidity can be a direct result of the global change due to certain anthropogenic activities. In turn, it can be one possible explanation of the observed tendency of OMZs becoming larger in size and emerging in a broader range of geographical locations[2,16,18].

With regard to the second point above, interestingly, coexistence of two OMZs has indeed been observed in several field studies[3,5,8,11,28,54]. The shallow OMZ is usually less pronounced compared to the deep OMZ, which is in good agreement with our modelling results. Coexistence of a shallow (around 100 m) and deep (400 m) oxygen minima have been observed in several field studies at various locations around the world, e.g. in the eastern tropical North Atlantic (cf. Fig. 2 in[5] and Fig. 6a in[28]). Slightly nonmonotonous dependence of the oxygen distribution on the water depth was observed in the Pacific at $21°S, 86°W$ (see Fig. 20 in[28]), with the shallow and deep minima located at about 300 m and 800 m, respectively. Vertical oxygen profile at another locations in the Pacific ($21°S, 71°W$) was found to show two OMZs too: a shallow one at 100-300 m and a deep one at 1200 m; see Fig. 4a in[8]. Typical southern California oxygen vertical profile shows shallow (around 150 m) and deep (500–800 m) minima; see Fig. 3.1.1 in[11]. Exact position of the oxygen minima in the water column therefore shows a considerable variability depending on the geographical location.

A question naturally arises as to what is the depth of the oxygen minimum predicted by our model. As is shown in Supplementary Information, the generic spatial scale of the system is about 1 m. However, the value of γ used in simulations (see Table 1) is about seven times smaller than its realistic value. That brings an extra factor of 1/7, so that one (dimensionless) unit of length in our model is approximately 14 cm. Our model predicts the position of OMZ at about 900 in dimensionless units; in physical (dimensional) units, it therefore corresponds to approximately 130 m, which appears to be in a reasonable agreement with field data on the position of the shallow maximum. Thus, while a comprehensive explanation of the water column structure would undoubtfully require careful consideration of all relevant factors including specific details of water mixing, oxygen transport and variable oxygen solubility at different water temperature, the apparent agreement between some of field data (as in the previous paragraph) and our model predictions is encouraging.

We emphasize that our model is conceptual and has been designed with the specific purpose to make an insight into the role that the oxygen production by phytoplankton may play in the formation of an OMZ. Thus, it deliberately leaves aside other important factors that can contribute to the OMZ formation and evolution. In particular, the dependence of water temperature on the depth is likely to be important, as temperature is known to be another factor that affects the rate of photosynthetic oxygen production[33,60]. Also, heterogeneity of the water temperature can affect vertical mixing, especially in the presence of thermocline. A more detailed model therefore has to include temperature explicitly as another factor controlling the OMZ properties. This should become a focus of future research.

Similarly, our choice of parameter values used in simulations is largely hypothetical and is not meant to represent any specific ocean conditions. However, we argue here that, because our model is conceptual and hence inevitably somewhat simplistic, looking for 'precise' parameter values would perhaps be excessive. Moreover, a preliminary search through the literature reveals that, while data on hydrophysical and geochemical processes (e.g. vertical mixing and turbidity) are abundant, biological data related to photosynthesis and oxygen production are scarce. Estimation of parameter values in the biological part of our model therefore poses a significant challenge that needs to be treated separately. This should become another focus of future work.

Data availability
This paper does not use or generate any data.

References
1. Devol, A. Vertical distribution of zooplankton respiration in relation to the intense oxygen minimum zones in two British Columbia fjords. *J. Plankton Res.* **3**, 593–602 (1981).
2. Gilly, W. F., Beman, J. M., Litvin, S. Y. & Robison, B. H. Oceanographic and biological effects of shoaling of the oxygen minimum zone. *Ann. Rev. Mar. Sci.* **5**, 393–420 (2013).
3. Pizarro, O. *et al.* Underwater glider observations in the Oxygen Minimum Zone off Central Chile. *Bull. Amer. Meteorol. Soc.* https://doi.org/10.1175/BAMS-D-14-00040.1 (2016).
4. Garçon, V. *et al.* Multidisciplinary observing in the world ocean's Oxygen Minimum Zone regions: From climate to fish-the VOICE initiative. *Front. Mar. Sci.* **6**, 722 (2019).
5. Hoving, H. J. T. *et al.* In situ observations show vertical community structure of pelagic fauna in the eastern tropical North Atlantic off Cape Verde. *Sci. Rep.* **10**, 21798 (2020).
6. Webb, P. *Introduction to Oceanography* (Roger Williams University, 2021).
7. Breitburg, D. *et al.* Declining oxygen in the global ocean and coastal waters. *Science* **359**, eaam7240 (2018).
8. Paulmier, A. & Ruiz-Pino, D. Oxygen minimum zones (OMZs) in the modern ocean. *Prog. Oceanogr.* **80**, 113–128 (2009).

9. Hahn, J., Brandt, P., Greatbatch, R. J., Krahmann, G. & Körtzinger, A. Oxygen variance and meridional oxygen supply in the Tropical North East Atlantic oxygen minimum zone. *Clim. Dyn.* **43**, 2999–3024 (2014).
10. Bretagnon, M. *et al.* Modulation of the vertical particle transfer efficiency in the oxygen minimum zone off Peru. *Biogeosciences* **15**, 5093–5111 (2018).
11. Pitcher, G. C. *et al.* System controls of coastal and open ocean oxygen depletion. *Prog. Oceanogr.* **197**, 102613 (2021).
12. Morrison, J. *et al.* The oxygen minimum zone in the Arabian Sea during 1995. *Deep Sea Res. Part II* **46**, 1903–1931 (1999).
13. Stramma, L., Johnson, G. C., Sprintall, J. & Mohrholz, V. Expanding oxygen-minimum zones in the tropical oceans. *Science* **320**, 655–658 (2008).
14. O'Boyle, S. *Oxygen Depletion in Coastal Waters and the Open Ocean* (CRC/Taylor and Francis, 2020). https://doi.org/10.1201/9780203704271-3.
15. Borges, F. O., Sampaio, E., Santos, C. P. & Rosa, R. Impacts of low oxygen on marine life: Neglected, but a crucial priority for research. *Biol. Bull.* **243**(2), 104–119 (2022).
16. Diaz, R. J. & Rosenberg, R. Spreading dead zones and consequences for marine ecosystems. *Science* **321**, 926–929 (2008).
17. Watson, A. J., Lenton, T. M. & Mills, B. Ocean deoxygenation, the global phosphorus cycle and the possibility of human-caused large-scale ocean anoxia. *Philos. Trans. A* **375**, 20160318 (2017).
18. Levin, L. A. Deep-ocean life where oxygen is scarce. *Am. Sci.* **90**, 436–444 (2002).
19. Oguz, T. Role of physical processes controlling oxycline and suboxic layer structures in the Black Sea. *Glob. Biogeochem. Cyc.* **16**(2), 1019 (2002).
20. Pena, M. A., Katsev, S., Oguz, T. & Gilbert, D. Modeling dissolved oxygen dynamics and hypoxia. *Biogeosciences* **7**, 933–957 (2010).
21. Bettencourt, J. H. *et al.* Boundaries of the Peruvian oxygen minimum zone shaped by coherent mesoscale dynamics. *Nat. Geosci.* **8**, 937–941 (2015).
22. Vergara, O. *et al.* Seasonal variability of the oxygen minimum zone off Peru in a high-resolution regional coupled model. *Biogeosciences* **13**, 4389–4410 (2016).
23. Andrews, O., Buitenhuis, E., Le Quéré, C. & Suntharalingam, P. Biogeochemical modelling of dissolved oxygen in a changing ocean. *Philos. Trans. R. Soc. A* **375**, 20160328 (2017).
24. Pizarro Koch, M. *et al.* Seasonal variability of the southern tip of the Oxygen Minimum Zone in the eastern South Pacific (30°-38° S): A modeling study. *J. Geophys. Res. Oceans* **124**, 8574–8604 (2019).
25. Bettencourt, J. H. *et al.* Effects of upwelling duration and phytoplankton growth regime on dissolved-oxygen levels in an idealized Iberian Peninsula upwelling system. *Nonlin. Processes Geophys.* **27**, 277–294 (2020).
26. Pizarro-Koch, M. *et al.* On the interpretation of changes in the subtropical oxygen minimum zone volume off Chile during two La Niña events (2001 and 2007). *Front. Mar. Sci.* **10**, 1155932 (2023).
27. Charpentier, J., Mediavilla, D. & Pizarro, O. Modeling the seasonal cycle of the oxygen minimum zone over the continental shelf off Concepción, Chile (36.5° S). *Biogeosci. Discuss.* **9**, 7227–7256 (2012).
28. Brandt, P. *et al.* On the role of circulation and mixing in the ventilation of oxygen minimum zones with a focus on the eastern tropical North Atlantic. *Biogeosciences* **12**, 489–512 (2015).
29. Keeling, R. F., Kortzinger, A. & Gruber, N. Ocean deoxygenation in a warming world. *Annu. Rev. Mar. Sci.* **2**, 199–229 (2010).
30. Helm, K. P., Bindoff, N. L. & Church, J. A. Observed decreases in oxygen content of the global ocean. *Geophys. Res. Lett.* **38**, L23602 (2011).
31. D'Avanzo, D. & Kremer, J. N. Diel oxygen dynamics and anoxic eutrophic estuary of Waquoit bay, Massachusetts. *Estuaries* **17**, 131–139 (1994).
32. Riedel, B., Zuschin, M., Haselmair, A. & Stachowitsch, M. Oxygen depletion under glass: Behavioural responses of benthic macrofauna to induced anoxia in the northern adriatic. *J. Exp. Mar. Biol. Ecol.* **367**, 17–27 (2008).
33. Levin, L. A. *et al.* Effects of natural and human-induced hypoxia on coastal benthos. *Biogeosciences* **6**, 2063–2098 (2009).
34. Riedel, B., Zuschin, M. & Stachowitsch, M. Tolerance of benthic macrofauna to hypoxia and anoxia in shallow coastal seas: a realistic scenario. *Mar. Ecol. Prog. Ser.* **458**, 39–52 (2012).
35. Smith, D. W. & Piedrahita, R. H. The relation between phytoplankton and dissolved oxygen in fish ponds. *Aquaculture* **68**, 249–265 (1988).
36. Yoshikawa, T., Murata, O., Furuya, K. & Eguchi, M. Short-term covariation of dissolved oxygen and phytoplankton photosynthesis in a coastal fish aquaculture site. *Estuar. Coast. Shelf Sci.* **74**, 515–527 (2007).
37. Xu, J. *et al.* Long-term and seasonal changes in nutrients, phytoplankton biomass, and dissolved oxygen in deep bay, Hong Kong. *Estuaries Coasts* **33**, 399–416 (2010).
38. Wang, J. & Zhang, Z. Phytoplankton, dissolved oxygen and nutrient patterns along a eutrophic river-estuary continuum: Observation and modeling. *J. Environ. Manag.* **261**, 110233 (2020).
39. Moss, B. R. *Ecology of Fresh Waters: Man and Medium, Past to Future* (Wiley, 2009).
40. Nababan, B., Ulfah, D. & Panjaitan, J. Light propagation, coefficient attenuation, and the depth of one optical depth in different water types. *IOP Conf. Ser. Earth Environ. Sci.* **944**, 012047 (2021).
41. Eppley, R. W. & Peterson, B. J. Particulate organic matter flux and planktonic new production in the deep ocean. *Nature* **282**, 677–680 (1979).
42. Bowers, D. & Brett, H. The relationship between CDOM and salinity in estuaries: An analytical and graphical solution. *J. Mar. Syst.* **73**, 1–7 (2008).
43. Sekerci, Y. & Petrovskii, S. Mathematical modelling of plankton-oxygen dynamics under the climate change. *Bull. Math. Biol.* **77**, 2325–2353 (2015).
44. Okubo, A. *Diffusion and Ecological Problems: Mathematical Models* (Springer, 1980).
45. Morris, I., Glover, H. E. & Yentsch, C. S. Products of photosynthesis by marine phytoplankton: The effect of environmental factors on the relative rates of protein synthesis. *Mar. Biol.* **27**, 1–9 (1974).
46. Mineeva, N. M., Korneva, L. G. & Solovyova, V. V. Influence of environmental factors on phytoplankton photosynthetic activity in the Volga river reservoirs. *Inland Water Biol.* **9**(3), 258–267 (2016).
47. McKinley, G. A., Follows, M. J. & Marshall, J. Interannual variability of the air-sea flux of oxygen in the North Atlantic. *Geophys. Res. Lett.* **27**(18), 2933–2936 (2000).
48. Gruber, N., Gloor, M., Fan, S.-M. & Sarmiento, J. L. Air-sea flux of oxygen estimated from bulk data: Implications for the marine and atmospheric oxygen cycles. *Glob. Biogeochem. Cycles* **15**(4), 783–803 (2001).
49. Morgan, E. J. *et al.* An atmospheric constraint on the seasonal air-sea exchange of oxygen and heat in the extratropics. *J. Geophys. Res. Oceans* **126**, e2021JC017510 (2021).
50. Richards, F. A. Oxygen in the ocean. In: *Treatise on Marine Ecology and Paleoecology* (ed. Hedgpeth, J. W.) 185–238 (1957).
51. Doney, S. C. & Steinberg, D. K. The ups and downs of ocean oxygen. *Nat. Geosci.* **6**, 515–516 (2013).
52. Mosch, T. *et al.* Factors influencing the distribution of epibenthic megafauna across the Peruvian oxygen minimum zone. *Deep-Sea Res.* **168**, 123–135 (2012).
53. Rapp, I. *et al.* Controls on redox-sensitive trace metals in the Mauritanian oxygen minimum zone. *Biogeosciences* **16**, 4157–4182 (2019).
54. Thomsen, S. *et al.* Remote and local drivers of oxygen and nitrate variability in the shallow oxygen minimum zone off Mauritania in June 2014. *Biogeosciences* **16**, 979–998 (2019).

55. Lazzari, P., Grimaudo, R., Solidoro, C. & Valenti, D. Stochastic 0-dimensional biogeochemical flux model: effect of temperature fluctuations on the dynamics of the biogeochemical properties in a marine ecosystem. *Commun. Nonlinear Sci. Numer. Simul.* **103**, 105994 (2021).
56. Naess, A. *Stochastic Dynamics of Marine Structures* (Cambridge University Press, 2012).
57. Paiva, V. *et al.* Overcoming difficult times: The behavioural resilience of a marine predator when facing environmental stochasticity. *Mar. Ecol. Prog. Ser.* **486**, 277–288 (2013).
58. Shim, W. J. & Thompson, R. C. Microplastics in the ocean. *Arch. Environ. Contam. Toxicol.* **69**, 265–268 (2015).
59. Zhou, Q. *et al.* Trapping of microplastics in halocline and turbidity layers of the semi-enclosed Baltic Sea. *Front. Mar. Sci.* **8**, 761566 (2021).
60. Robinson, C. Plankton gross production and respiration in the shallow water hydrothermal systems of Milos, Aegean Sea. *J. Plankt. Res.* **22**, 887–906 (2000).

Acknowledgements

Author contributions

Y.A.: Formal analysis, Software, Visualization, Validation, Writing - original draft. I.S.: Formal analysis, Investigation, Validation, Visualization, Writing - original draft. S.P.: Conceptualization, Methodology, Formal analysis, Investigation, Validation, Supervision, Writing - original draft, Writing - review & editing.

Competing interests

The authors declare no competing interests.

Additional information

Supplementary Information The online version contains supplementary material available at https://doi.org/10.1038/s41598-024-72207-3.

Correspondence and requests for materials should be addressed to Y.A. or S.P.

Reprints and permissions information is available at www.nature.com/reprints.

Publisher's note Springer Nature remains neutral with regard to jurisdictional claims in published maps and institutional affiliations.